

**Titre:** Modeling carbon black reinforcement in rubber compounds  
Title:

**Auteurs:** Axel Van de Walle, Claude Tricot, & Michel Gerspacher  
Authors:

**Date:** 1994

**Type:** Rapport / Report

**Référence:** Van de Walle, A., Tricot, C., & Gerspacher, M. (1994). Modeling carbon black reinforcement in rubber compounds. (Rapport technique n° EPM-RT-94-17).  
Citation: <https://publications.polymtl.ca/9717/>

## Document en libre accès dans PolyPublie

Open Access document in PolyPublie

**URL de PolyPublie:** <https://publications.polymtl.ca/9717/>  
PolyPublie URL:

**Version:** Version officielle de l'éditeur / Published version

**Conditions d'utilisation:** Tous droits réservés / All rights reserved  
Terms of Use:

## Document publié chez l'éditeur officiel

Document issued by the official publisher

**Institution:** École Polytechnique de Montréal

**Numéro de rapport:** EPM-RT-94-17  
Report number:

**URL officiel:**  
Official URL:

**Mention légale:**  
Legal notice:

19 SEP. 1994

**EPM/RT-94/17**

**MODELING CARBON BLACK REINFORCEMENT  
IN RUBBER COMPOUNDS**

gratuit

*Axel Van de Walle, étudiant 2<sup>e</sup> cycle  
Claude Tricot, Ph.D.  
Michel Gerspacher, Ph.D.*

*Département de mathématiques appliquées*

*École Polytechnique de Montréal*

*mai 1994*

*Tous droits réservés. On ne peut reproduire ni diffuser aucune partie du présent ouvrage, sous quelque forme que ce soit, sans avoir obtenu au préalable l'autorisation écrite des auteurs.*

*Dépôt légal, mai 1994  
Bibliothèque nationale du Québec  
Bibliothèque nationale du Canada*

*Pour se procurer une copie de ce document, s'adresser:*

*Les Éditions de l'École Polytechnique  
École Polytechnique de Montréal  
Case postale 6079, Succursale Centre-ville  
Montréal (Québec) H3C 3A7  
Téléphone: (514) 340-4473  
Télécopie: (514) 340-3734*

*Compter 0,10 \$ par page et ajouter 3,00 \$ pour la couverture, les frais de poste et la manutention. Régler en dollars canadiens par chèque ou mandat-poste au nom de l'École Polytechnique de Montréal.*

*Nous n'honorerons que les commandes accompagnées d'un paiement, sauf s'il y a eu entente préalable dans le cas d'établissements d'enseignement, de sociétés ou d'organismes canadiens.*

# 1 Introduction

Our study of the effect of carbon black used as a filler in polymers is based on:

- a simple mechanical model representing the elementary interactions between two agglomerates;
- a statistical description of the agglomerates that models the collective behavior of a group of agglomerates.

Our goal is to explain and model the typical variation of the complex Coulomb modulus as a function of amplitude of deformation (see figure 1).

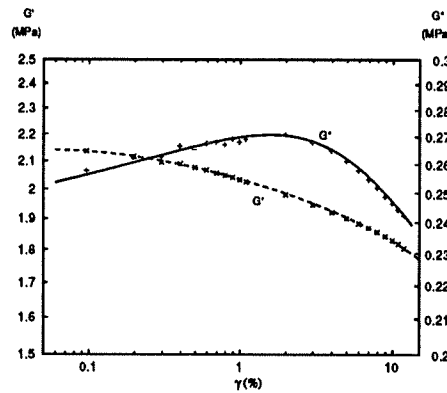


Figure 1: Typical relation between Coulomb modulus and amplitude of deformation

We will first describe the general simplifications we made in our model before exposing the mechanical model itself. Our statistical description of a collection of elementary mechanical model will then yield a behavior which compares favorably with experimental results.

## 2 General Hypotheses of the Model

The Coulomb modulus is assumed to be the sum of two contributions:

- the perfectly linear viscoelastic behavior of the polymer;
- the effect of carbon black agglomerates.

We will focus on the second contribution, the first being well-known.

The way carbon black agglomerates are embedded in a polymer matrix can be represented by figure 2 (a). The polymer strings being much smaller than the agglomerates, the polymer matrix can be considered as a viscoelastic continuum.

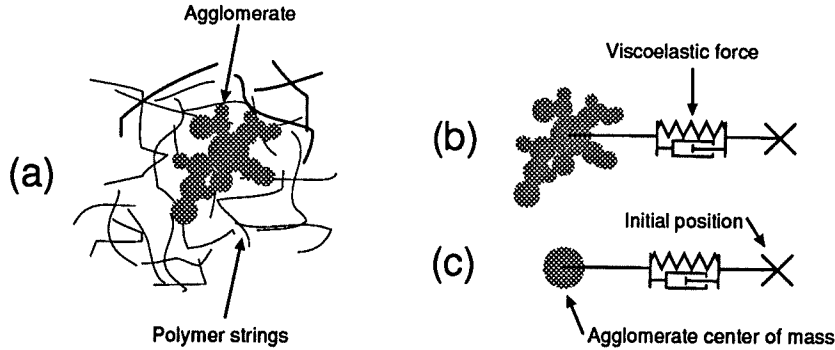


Figure 2: Polymer-agglomerate Interaction

This continuum tends to bring the agglomerates to their rest positions. Since the polymer is a linear medium, the sum of all strain exerted on an agglomerate can be represented by a linear spring-damper system (b) linking the agglomerate to its rest position (represented by a cross). Considering only the position of the center of mass of the agglomerates with respect to its rest position, the system reduces to (c).

The material is composed of many of these agglomerates, all of which can be represented by the same simple mechanical model. But when numerous agglomerates are brought nearby, another force acts on the agglomerates: the London-van der Waals interaction due to neighbouring agglomerates.

The effect of stretching the polymer is equivalent to moving the rest positions farther from each other. To evaluate the position of these new rest positions, we can interpolate linearly, as shown in figure 3 (a) and (b). Notice that because there is a force acting between them, the agglomerates do not necessarily remain in their rest positions when the polymer is stretched.

### 3 Microscopic Interaction Between Aggregates

In this section we will derive an expression that describes the forces which act on the agglomerates. But first we need to make some more simplifying assumptions.

The London-van der Waals interaction binding the agglomerates is theoretically of infinite range but since its magnitude decreases as the seventh power of the distance, its effect rapidly vanishes. This enables us to focus only on the interactions between almost touching agglomerates.

We also assume that the interaction between two agglomerates does not influence the behavior of other agglomerates. The problem can thus be considered a sum of  $N$  two-body problems instead of a  $2N$ -body problem. The independence of each two-body problem eases their statistical analysis without

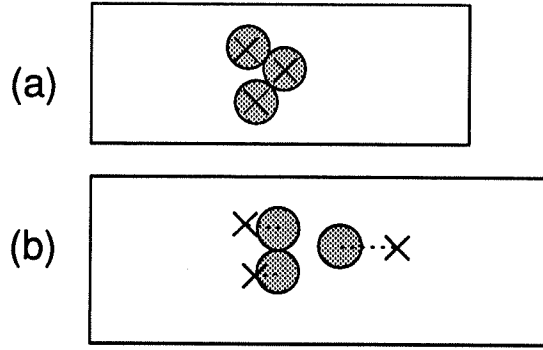


Figure 3: Agglomerates (in gray) and equilibrium positions (crosses) under no deformation (a) and when the polymer is stretched (b).

introducing too many artefacts, as we will see later on.

The microscopic mechanical model then reduces to figure 4 (a). Two spring-damper systems placed in serie can be replaced one equivalent spring-damper system (b). Only remains a string of a spring-damper system (representing the polymer-agglomerate interaction) and a non-linear elastic spring (representing the London-van der Waals force).

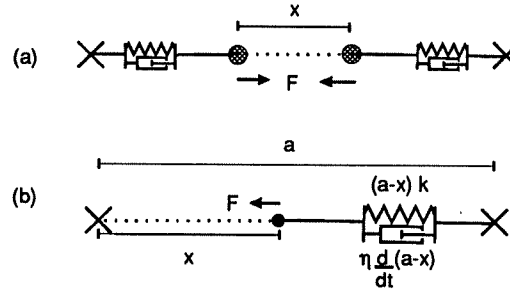


Figure 4: Microscopic mechanical model.  $k$  is the elastic constant,  $\eta$  the viscous constant and  $F$  the force between the two agglomerates.

To model the interaction between the two agglomerates, we can use the expression of the London-van der Waals force which has both an attractive term due to the van der Waals force, and a repulsive term accounting for the repulsion between electrons. The exact expression  $F(x)$  of this force is however dependent on the exact shape of the agglomerates. This shape greatly varies, but in any cases, there is always a region where the force increases (for small distances) and an region where the force decreases (for large distances), as shown in figure 5. These descriptive properties are sufficient for our qualitative model.

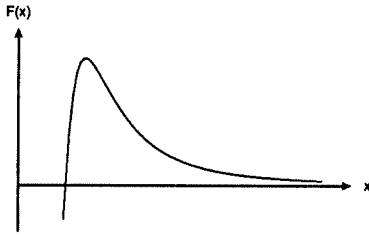


Figure 5: The typical shape of the force  $F$  between agglomerates as a function of distance  $x$ .

By inspection of figure 4 (b) one can find the equations of movement for  $x$ , the agglomerate position as a function of time. Since

$$F_{\text{elastic}} + F_{\text{viscous}} - F_{\text{London-van der Waals}} = m \frac{d^2x}{dt^2}$$

where  $m$  is the agglomerate mass, then

$$(a - x)k + \eta \frac{d}{dt}(a - x) - F(x) = m \frac{d^2x}{dt^2}$$

where  $\eta$  is the viscous constant,  $k$ , the spring constant, and  $a$ , the distance between the rest positions.

We now seek to plot the curve of  $F$  versus  $a$ . Suppose that the variation of  $a$  is sufficiently slow so that the system has always the time to reach a stationnary state (*i.e.* the process is quasi-static). One must recall that the viscoelastic properties we want to model persist at frequencies as low as 1 hertz. During such slow movement, the composite must have plenty of time to reach equilibrium.

Under the quasi-static assumption, both the  $\eta \frac{d}{dt}(a - x)$  and the  $m \frac{d^2x}{dt^2}$  terms are negligibly small compared to  $(a - x)k - F(x)$ . So the equation simply reduces to the conditions of static equilibrium:

$$(a - x)k = F(x)$$

This equation can be solved graphically by finding the value  $F$  at which the curves  $F(x)$  and  $(a - x)k$  intersect, for each value of  $a$ . Figure 6 shows different possible points of intersection.

- (a) When no strain is applied on the polymer,  $a = a_0$  and the equilibrium position  $x$  lies in the increasing region of  $F$ .
- (b) When  $a$  is brought up to a critical value  $a_b$ , a second stable equilibrium point appears while the first one disappears. Since there is a rapid jump from one point to another, the London-van der Waals link between the agglomerates is said to “break”.

- (c) For large values of  $a$ , the equilibrium point lies in the decreasing region of  $F$ .
- (d) When  $a$  decreases down to a critical value  $a_b - \Delta a$ , another jump from one equilibrium to a new one occurs. The London-van der Waals link between the agglomerates “reforms”.
- (e) At low values of  $a$ , the equilibrium position again lies in the increasing region of  $F$ .

Figure 7 shows the complete curve that can be obtained by this method. The particular values of  $a$  used in figure 6 are marked by heavy dots.

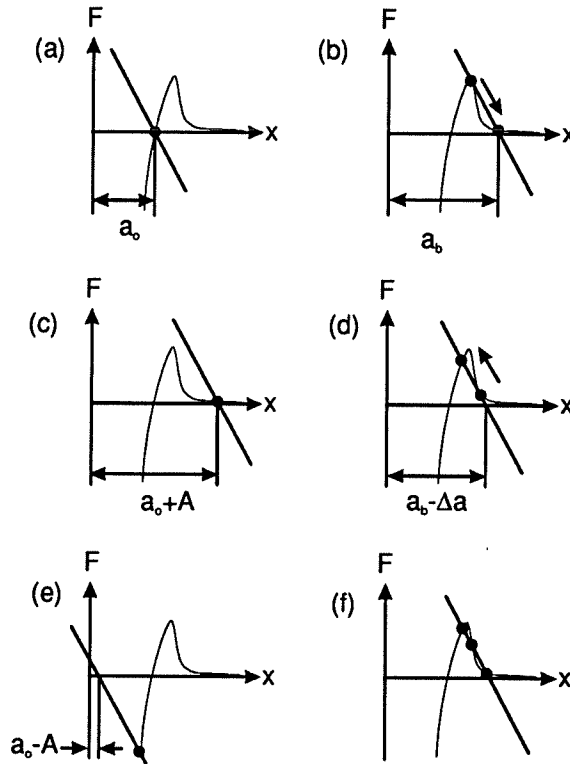


Figure 6: Graphical determination of  $F$  versus  $a$ .

Notice the appearance of a hysteresis cycle whose surface gives the energy loss. One may wonder where is the physical origin of the energy loss since the viscous term has been neglected in our derivation. During the fast transition between two equilibrium points, the quasi-static assumption does no longer hold: the viscous force becomes significant and creates great energy losses while

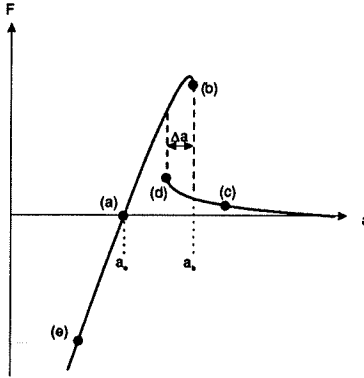


Figure 7: Hysteresis curve of  $F$  versus  $a$ .

the agglomerate converges toward the new equilibrium. Despite of that, the quasi-static assumption is a good approximation because:

- the transition is fast and the quasi-static assumption is violated during an infinitesimal amount of time;
- the main effect of the viscous force is to prevent the agglomerate from oscillating around its new equilibrium position;
- since energy is conserved, the energy dissipation due to the viscous force must equal the area of the hysteresis cycle.

The viscous term is implicitly taken into account by the appearance of a hysteresis cycle.

One might also be concerned by a third equilibrium point (see figure 6 (f)) that we neglected. This point is unstable, as it can be shown from the slope of each curve at the point of intersection.

Let us notice that the exact expression of  $F(x)$  is not important. For the qualitative behavior of our model to be correct, the only requirements are that  $F(x)$  has:

- an increasing and a decreasing region;
- an interval where  $-\frac{dF(x)}{dx} > -k$ .

Let us now consider qualitatively what happens at different amplitudes of sinusoidal deformation (see figure 8).

- At low amplitudes, the deformation is insufficient for the system to reach the critical point where hysteresis appears (a). Energy losses are low and so  $G''$  is small.  $G'$  is large since the slope of  $F$  is steep.

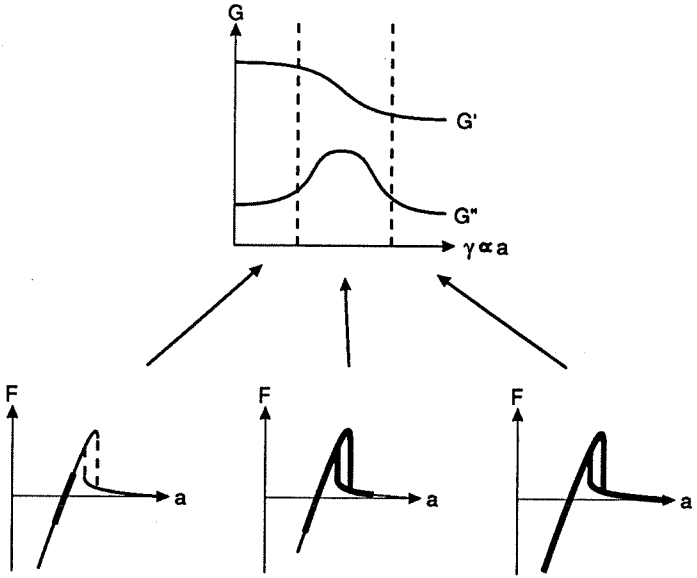


Figure 8: Explanation of the amplitude dependence of  $G'$  and  $G''$ .

- At moderate amplitudes, the hysteresis appears, and increased energy loss causes  $G''$  to increase. Since the average slope of  $F$  decreases,  $G'$  also decreases.
- At high amplitudes, the losses do not increase much, because they are mainly produced by the hysteresis cycle, which keeps the same area. But since

$$(\text{Energy losses}) \propto G''(\text{Amplitude})^2$$

an increased amplitude at constant energy loss yields a decrease of  $G''$ .

Until now, we have only considered the behavior of a pair of agglomerates and qualitatively described how this behavior influences the values of  $G'$  and  $G''$  at different amplitudes. In the next section, we will derive an expression of the contribution of a pair of agglomerates to the Coulomb modulus.

## 4 Idealized Response of the Microscopic Model

In order to make our statistical description more manageable mathematically, we must first construct an idealized version of the mechanical model. Under a small deformation, the distance  $a$  between rest positions is assumed to be linearly related to the shear strain  $\gamma$ :

$$a = a_o(1 + r\gamma)$$

which becomes, under a sinusoidal deformation,

$$a = a_0(1 + r\gamma_0 \sin \omega t)$$

where  $r$  is parameter depending on the spatial orientation of a given agglomerate pair. The plot of  $F$  versus  $\gamma$  is thus similar to figure 7. If we also linearize each curved portion of the curve, we obtain figure 9. Here follows a derivation of the complex viscoelastic constant  $g = g' + ig''$  of this idealized elementary mechanical model.

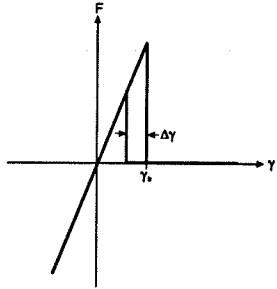


Figure 9: Idealized Response as a function of  $\gamma$

If  $F$  were linear, we would have

$$F = g\gamma$$

but we just saw that  $F$  is not linear so only an *effective* value of  $g$  can be found. This *effective* value is defined as the first term of the Fourier series of  $F$  as a function of time, when  $\gamma = \gamma_0 e^{i\omega t}$ . We will use an alternative approach giving an estimate of  $g$  without relying to Fourier series.

Let us first consider the imaginary part of  $g$ . The energy loss  $E_l$  as a function of amplitude  $\gamma_0$  gives a step function centered on the onset of the hysteresis cycle at  $\gamma_0 = \gamma_b$  (see figure 10 (a)). Recalling that

$$G'' \propto \frac{E_l}{\gamma_0^2}$$

we find, analogously:

$$g''(\gamma_0, \gamma_b) = \begin{cases} 0 & \text{if } \gamma_0 \leq \gamma_b \\ \frac{E_l}{\gamma_0^2} & \text{if } \gamma_0 > \gamma_b \end{cases}$$

Figure 10 (b) shows  $g''$  as a function of  $\gamma_0$ . The area enclosed by the hysteresis cycle can be expressed as

$$E_l \approx g_0 \gamma_b \Delta\gamma$$

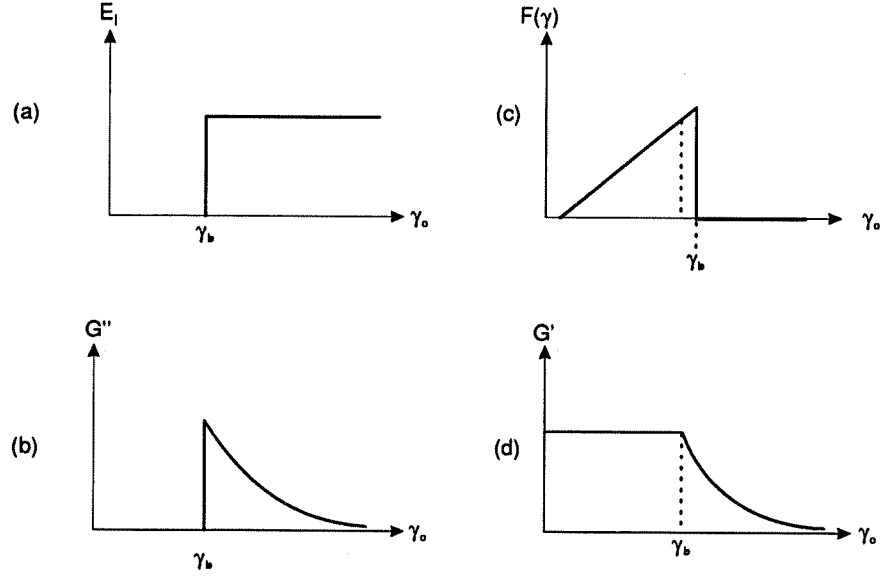


Figure 10: Idealized microscopic viscoelastic constants

where  $g_0$  is the slope of the increasing region of  $F$  versus  $\gamma$  and  $\Delta\gamma$  is the width of the hysteresis cycle.

An estimate of the effective  $g'$  is obtained by computing a linear regression of  $F$  versus  $\gamma$  on the interval  $[0, \gamma_o]$ . (A more rigorous treatment would require to consider the interval  $[-\gamma_o, \gamma_o]$  instead. But it would only adds a constant amplitude-independant contribution to  $g'$ .) If we assume that the width of the hysteresis cycle is small, the curve  $F$  versus  $\gamma$  reduces to the graph  $F(\gamma)$  shown in figure 10 (c). For  $\gamma_o \leq \gamma_b$ , the regression yields a slope of  $g_0$  while for  $\gamma_o > \gamma_b$  the slope is given by:

$$g'(\gamma_o, \gamma_b) \approx \frac{\int_0^{\gamma_o} \gamma F(\gamma) d\gamma}{\int_0^{\gamma_o} \gamma^2 d\gamma} = \frac{\int_0^{\gamma_b} \gamma F(\gamma) d\gamma}{\frac{\gamma_b^3}{3}} = \frac{\int_0^{\gamma_b} g_0 \gamma^2 d\gamma}{\frac{\gamma_b^3}{3}} = \frac{g_0 \gamma_b^3}{\gamma_b^3}$$

In summary, the idealized description of the microscopic viscoelastic constant as a function of  $\gamma_o$ , is:

$$g(\gamma_o, \gamma_b) = g_0 s'(\gamma_o, \gamma_b) + i g_0 \left( \frac{\Delta\gamma}{\gamma_b} \right) s''(\gamma_o, \gamma_b)$$

where

$$s'(\gamma_o, \gamma_b) = \begin{cases} 1 & \text{if } \gamma_o \leq \gamma_b \\ \frac{\gamma_b^3}{\gamma_o^3} & \text{if } \gamma_o > \gamma_b \end{cases} \quad \text{and} \quad s''(\gamma_o, \gamma_b) = \begin{cases} 0 & \text{if } \gamma_o \leq \gamma_b \\ \frac{\gamma_b^2}{\gamma_o^2} & \text{if } \gamma_o > \gamma_b \end{cases}$$

Figure 10 (b) et (d) show the real and imaginary part of  $g(\gamma_o, \gamma_b)$ .

## 5 Statistical Description

It seems that the idealized response derived in the last section yields a behavior too discontinuous to compare favorably with experimental results. But one must recall that the composite is made of many pairs of agglomerate, each of which breaks and reforms at different times in the cycle. The resulting macroscopic response  $G(\gamma)$  is then a smoothed version of  $g(\gamma, \gamma_b)$  as shown in figure 11.

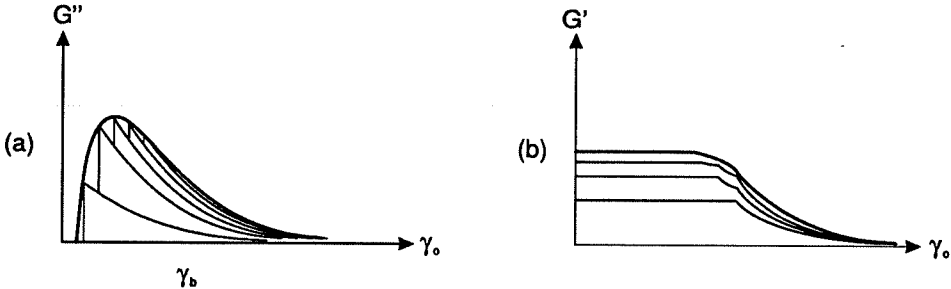


Figure 11: The smoothing effect of distributed values of  $\gamma_b$

We identified two major causes of smoothing:

- During uniaxial or shear deformation, the relative displacement of the pairs of agglomerates is dependent on the orientation of the pair. So a given macroscopic deformation produces a range of values of microscopic deformation.
- The binding energy of the van der Waals links is not constant: for a given microscopic deformation, some pairs break, other do not.

These two effects give rise to two distributions that are convoluted together to yield a single distribution function. Let  $N(\gamma_b)d\gamma_b$  be that function which gives the number of links that break when the polymer is stretched from  $\gamma_b$  to  $\gamma_b + d\gamma_b$ . The complex Coulomb modulus is then given by:

$$G(\gamma) = \int_0^\infty g_0(\gamma_b)s'(\gamma, \gamma_b)N(\gamma_b)d\gamma_b + i \int_0^\infty g_0(\gamma_b)hs''(\gamma, \gamma_b)N(\gamma_b)d\gamma_b$$

where  $h$  is the average value of  $\frac{\Delta\gamma}{\gamma_b}$ . By taking the average value of the ratio  $\frac{\Delta\gamma}{\gamma_b}$  we assume that  $h$  follows a distribution which is independent of  $\gamma_b$ . Under the same assumption, we can factor  $h$  out of the integral.

Note that the effect of  $g_0(\gamma_b)$  is undistinguishable from the one of  $N(\gamma_b)$  because the effect of a great number of weak links is undistinguishable from the one of a small number of strong links. We then combine  $g_0(\gamma_b)$  and  $N(\gamma_b)$  into one weighting function:

$$W(\gamma_b) = g_0(\gamma_b)N(\gamma_b)$$

The system then reduces to:

$$G(\gamma) = \int_0^\infty s'(\gamma, \gamma_b)W(\gamma_b)d\gamma_b + ih \int_0^\infty s''(\gamma, \gamma_b)W(\gamma_b)d\gamma_b$$

This equation completely describes the system. The exact forms of  $s'(\gamma, \gamma_b)$  and  $s''(\gamma, \gamma_b)$  are known but

- the constant  $h$  and
- the function  $W(\gamma_b)$

have yet to be determined from experimental data.

$G'(\gamma)$  and  $G''(\gamma)$  are expressed as the convolution of the same weighting function  $W(\gamma_b)$  with known functions  $s'(\gamma, \gamma_b)$  and  $s''(\gamma, \gamma_b)$ . This helps to explain why there is a very similar relation between  $G'$  and  $G''$  for different carbon black composites. The functions  $s'(\gamma, \gamma_b)$  and  $s''(\gamma, \gamma_b)$  remain the same for any material having the kind of dissipation mechanism we described here. On the other hand,  $W(\gamma_b)$  is dependent on the precise type of composite.

We can now see why the two-body assumption introduced in section 3 does not alter the validity of our model. It is true that the breakage of one van der Waals link may change the force acting between other pairs of agglomerates. However, this will only change the value  $\gamma_b$  at which other pairs will break: functions  $s'(\gamma, \gamma_b)$  and  $s''(\gamma, \gamma_b)$  remain unaffected while the distribution  $W(\gamma_b)$  can be adjusted to take this possibility into account.

What can be done now to test this model? After all, the unknown function  $W(\gamma_b)$  gives us an infinite number of degrees of freedom. It is indeed easy to find a  $W(\gamma_b)$  such that  $G''(\gamma)$  fits experimental data. But then, for the same  $W(\gamma_b)$ ,  $G'(\gamma)$  has to fit also. The criterion that  $G'(\gamma)$  and  $G''(\gamma)$  must both fit gives us the ultimate test of our model. Preliminary results indicate that this is actually the case (see figures 12 through 15).

To obtain these figures, we use the graph of  $G''(\gamma)$  to find the function  $W(\gamma_b)$ . If we express our integrals as a finite sums, the process reduces to the simple problem of solving a finite system of linear equations. We then compute  $G'(\gamma)$  from  $W(\gamma_b)$ , again using discrete integrals. The value of  $h$  is finally adjusted to give the best fit.

For that procedure to work, one must first subtract the constant contribution of the polymer (noted  $G_p = G'_p + iG''_p$ ) from the values of  $G'$  and  $G''$ . The horizontal lines on the graphs of  $G'$  and  $G''$  show the values used in the computations. Why is the value of  $G''_p$  so low and the value of  $G'_p$  so high? Because the insertion of inert and rigid particles (having a high  $G'$  and a negligible  $G''$ ) produces an increase of  $G'$  and a decrease of  $G''$ . So far, we modeled the effect of the interaction between carbon black agglomerates, but carbon black also behaves as a rigid and inert filler. This explains why carbon black also modifies the constant contribution to  $G$  usually attributed to the polymer only. Carbon black is quite rigid (yielding an increase of  $G'_p$ ), and purely elastic (yielding a decrease of  $G''_p$ ).

## 6 Conclusion

Here are the most important steps of the derivation of our model:

- Two phenomena contribute to the Coulomb modulus: the linear viscoelastic behavior of the polymer matrix, and the non-linear elastic behavior of carbon black.
- Upon deformation, the polymer pulls the agglomerate apart while the London-van der Waals force pushes them together.
- Because of the particular shape of the London-van der Waals force, two stable equilibrium points are possible for a pair of agglomerate: they can be “bound” or “unbound”.
- The transition from the bound to unbound state is the cause of  $G'$  decrease when  $\gamma$  increases.
- The high speed at which the transition from bounded to unbouded state occurs produces increased energy loss. This is the cause of the peak in the plot of  $G''$  versus  $\gamma$ .
- An expression of the viscoelastic constant of the idealized model of a pair of agglomerates can be found. Its real and imaginary parts, respectively, are proportionnal to:

$$s'(\gamma, \gamma_b) = \begin{cases} 1 & \text{if } \gamma \leq \gamma_b \\ \frac{\gamma^3}{\gamma_b^3} & \text{if } \gamma > \gamma_b \end{cases}$$

$$s''(\gamma, \gamma_b) = \begin{cases} 0 & \text{if } \gamma \leq \gamma_b \\ \frac{\gamma_b^2}{\gamma^2} & \text{if } \gamma > \gamma_b \end{cases}$$

where

- $\gamma$  is the amplitude of sinusoidal shear deformation;
- $\gamma_b$  is the amount of deformation causing the pair to unbind.

- The composite is made of a collection of those elementary models, each having a different  $\gamma_b$ . We then express the Coulomb modulus of the material as:

$$G(\gamma) = \int_0^\infty s'(\gamma, \gamma_b)W(\gamma_b)d\gamma_b + ih \int_0^\infty s''(\gamma, \gamma_b)W(\gamma_b)d\gamma_b$$

where

- $W(\gamma_b)$  is a weighting function giving the contribution of agglomerate pairs which break at  $\gamma = \gamma_b$  and

- $h$  is a constant proportionnal to the average width  $\Delta\gamma$  of the hysteresis cycle.
- With this expression, one can see why plots of  $G''$  versus  $G'$  for different polymers are so similar. The expression of  $s'$  and  $s''$  are universal, while  $W(\gamma_b)$  is material-dependent. There is a link between  $G'$  and  $G''$  because they are derived from the convolution of the same function  $W(\gamma_b)$ . The link remains accross different materials because  $s'(\gamma, \gamma_b)$  and  $s''(\gamma, \gamma_b)$  are material-independent.
- This model can be easily tested by showing that there exists a function  $W(\gamma_b)$  such that  $G'(\gamma)$  and  $G''(\gamma)$  can be both made to fit experimental data.

What still remains to be done is to:

- test the validity of the model over a wider range of experimental results;
- develop a precise expressions for  $W(\gamma_b)$ .

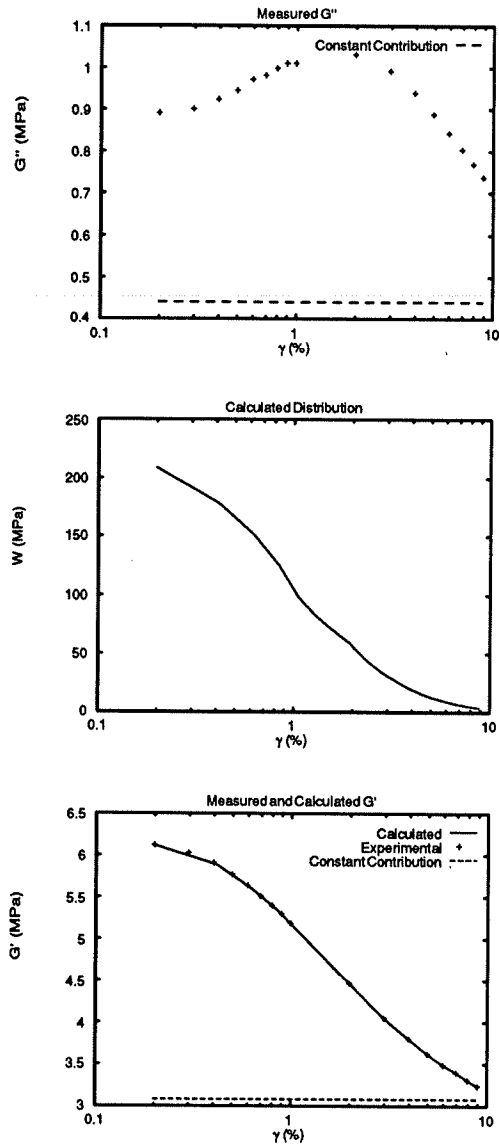


Figure 12: From top to bottom: experimental values of  $G''(\gamma)$  for SBR/N110 composite; Computed values of  $W(\gamma_b)$  for SBR/N110 composite; Computed and experimental values of  $G'(\gamma)$  for SBR/N110 composite.

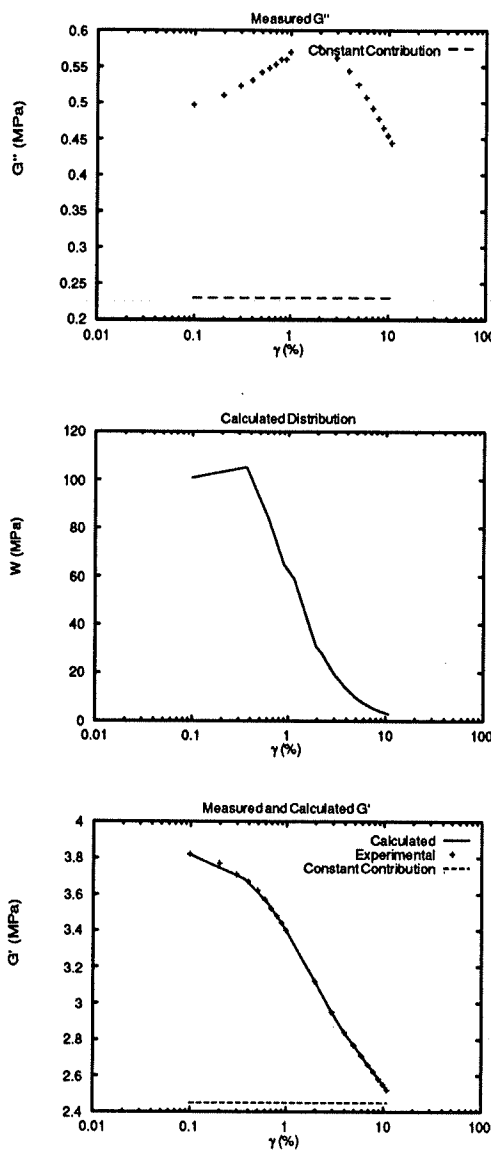


Figure 13: From top to bottom: experimental values of  $G''(\gamma)$  for SBR/N330 composite; computed values of  $W(\gamma_b)$  for SBR/N330 composite; computed and experimental values of  $G'(\gamma)$  for SBR/N330 composite.

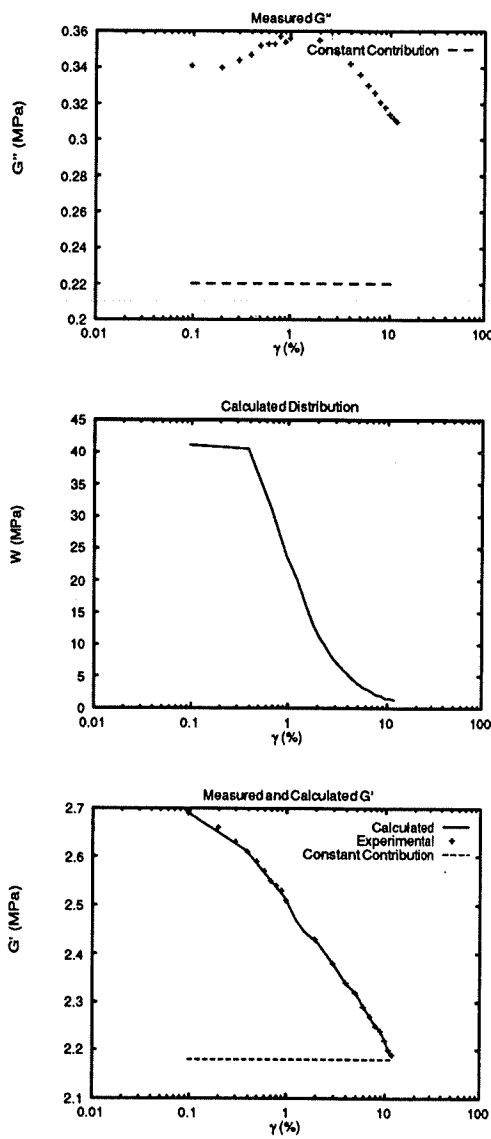


Figure 14: From top to bottom: experimental values of  $G''(\gamma)$  for SBR/N550 composite; computed values of  $W(\gamma_b)$  for SBR/N550 composite; computed and experimental values of  $G'(\gamma)$  for SBR/N550 composite.

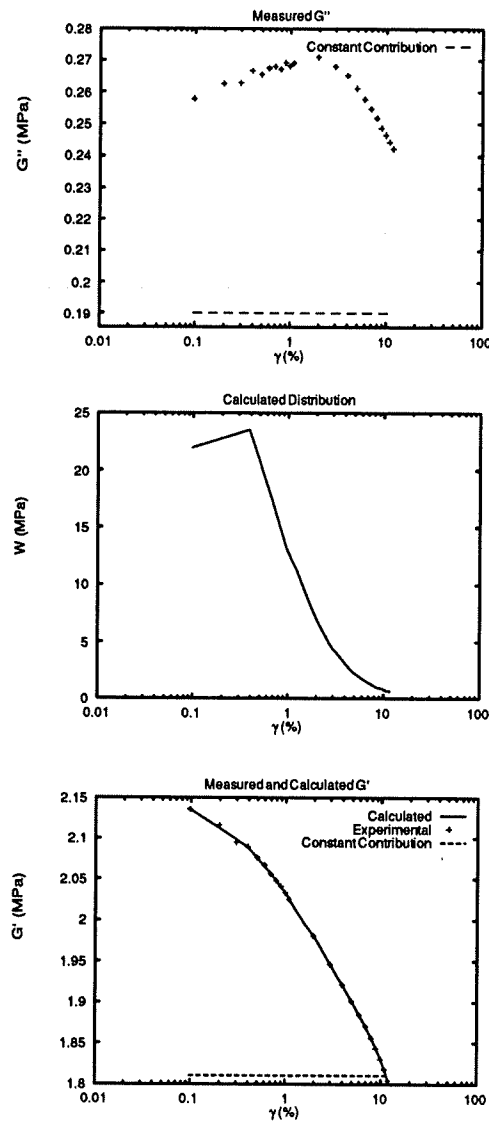


Figure 15: From top to bottom: experimental values of  $G''(\gamma)$  for SBR/N762 composite; computed values of  $W(\gamma_b)$  for SBR/N762 composite; computed and experimental values of  $G'(\gamma)$  for SBR/N762 composite.

ÉCOLE POLYTECHNIQUE DE MONTRÉAL



3 9334 00289876 3